Phys Chem Minerals (2015) 42:579–585
DOI 10.1007/s00269-015-0745-x

ORIGINAL PAPER

Raman spectra of stronadelphite $Sr_5(PO_4)_3F$ at high pressures

Shuangmeng Zhai[1] · Sean R. Shieh[2] · Weihong Xue[1] · Tianqi Xie[2]

Received: 11 February 2015 / Accepted: 25 March 2015 / Published online: 1 April 2015
© Springer-Verlag Berlin Heidelberg 2015

Abstract The Raman spectra of synthetic stronadelphite, $Sr_5(PO_4)_3F$, were investigated up to 21.1 GPa using a diamond anvil cell at room temperature. The new splittings of the PO_4 asymmetric stretching $\nu_{3b}(A_g)$ and bending $\nu_{4b}(A_g)$ vibrations were observed during compression. The Raman frequencies of all observed bands for stronadelphite continuously increase with increasing pressure. The quantitative analysis of pressure dependences of Raman bands indicates that the ν_3 asymmetric and ν_1 symmetric stretching vibrations show larger pressure coefficients (from 3.33 to 5.20 cm^{-1}/GPa), whereas the ν_4 and ν_2 bending vibrations have smaller pressure coefficients (from 1.35 to 1.96 cm^{-1}/GPa), which may be attributed to the pressure-induced structural evolution of PO_4 tetrahedron in stronadelphite at high pressure. The external modes show larger pressure coefficient from 3.47 to 6.41 cm^{-1}/GPa. The pressure coefficients of the PO_4 internal modes lead to the isothermal mode Grüneisen parameters varying from 0.214 to 0.449, which yields an average mode Grüneisen parameter of 0.332. On the other hand, those of the external modes give the isothermal mode Grüneisen parameters from 1.53 to 1.91. Therefore, the external mode Grüneisen parameters mainly contribute to the bulk Grüneisen parameters.

Keywords Stronadelphite · $Sr_5(PO_4)_3F$ · Raman spectra · High pressure

✉ Shuangmeng Zhai
zhaishuangmeng@vip.gyig.ac.cn

[1] Key Laboratory of High-temperature and High-pressure Study of the Earth's Interior, Institute of Geochemistry, Chinese Academy of Sciences, Guiyang 550002, Guizhou, China

[2] Department of Earth Sciences, University of Western Ontario, London, ON N6A 5B7, Canada

Introduction

Apatite is an important accessory phase and the most abundant phosphate mineral on Earth. The unique structure and chemistry of apatite allow for numerous substitutions of metal cations for Ca^{2+} (Hughes and Rakovan 2002; Pan and Fleet 2002) and therefore yield a great number of apatite-group minerals (Huminicki and Hawthorne 2002; White et al. 2005; Pasero et al. 2010; Kampf and Housley 2011; Biagioni and Pasero 2013). Due to the same charge and preferred coordination geometry and minor difference in the radius, Sr^{2+} can easily substitute Ca^{2+} in apatite to form solid solutions, which was confirmed in some minerals, e.g., fluorstrophite $SrCaSr_3(PO_4)_3F$ (Klevtsova 1964) and fluorcaphite $SrCaCa_3(PO_4)_3F$ (Khomyakov et al. 1997). If all Ca^{2+} cations in fluorapatite, $Ca_5(PO_4)_3F$, are substituted by Sr^{2+}, an isostructural compound of $Sr_5(PO_4)_3F$ can be obtained, as reported by Kreidler and Hummel (1970). Indeed, a new apatite-group mineral, stronadelphite, with an abbreviated chemical formula of $Sr_5(PO_4)_3F$ was found and reported by Pekov et al. (2010).

$Sr_5(PO_4)_3F$ was widely used as a host for rare earth dopants with subsequent applications as fluorescent and laser materials (DeLoach et al. 1994; Wang et al. 1996; Gloster et al. 1998; Brenier Brinier 2001; Schaffers 2004; Fang et al. 2008; Nagpure et al. 2011; Qiao and Seo 2014). Recently the compressibility and thermal expansivity of $Sr_5(PO_4)_3F$ were studied by X-ray diffraction measurements (He et al. 2013). Raman spectroscopy is another important technique for characterizing materials. Raman spectra of fluorapatite ($Ca_5(PO_4)_3F$) have been investigated under high pressures in previous studies (Williams and Knittle 1996; Comodi et al. 2001a). Williams and Knittle (1996) observed six internal modes up to above 15 GPa, and only one ν_3 mode was observable to about 25 GPa. On

the other hand, Comodi et al. (2001a) observed five lattice modes and 11 internal modes, but the pressure was limited to about 7 GPa. However, little information about the vibrational behavior of the stronadelphite $Sr_5(PO_4)_3F$ under compression is available.

In this paper, we report the first high-pressure micro-Raman spectroscopic study on the stronadelphite up to 21.1 GPa using a diamond anvil cell. The study has been performed over the frequency range from 200 to 1200 cm^{-1}. The effect of pressure on the characteristic Raman active internal PO_4^{3-} modes and some external modes of stronadelphite is analyzed. Combined with previous result of compressibility, the isothermal mode Grüneisen parameters were calculated and compared with other phosphate and silicate minerals.

Experimental

High-purity stronadelphite $Sr_5(PO_4)_3F$ sample was prepared by solid-state reactions from $NH_4H_2PO_4$, $SrCO_3$, and SrF_2. Reagent-grade $NH_4H_2PO_4$, $SrCO_3$, and SrF_2 powders were mixed in the proportion corresponding to the $Sr_5(PO_4)_3F$ stoichiometry, and the mixture was ground for 2 h in an agate mortar and pressed into pellets with a diameter of 5 mm under a uniaxial pressure of 30 MPa. The pellets were first sintered at 1273 K for 36 h, and then ground and calcined at 1273 K for 36 h again, to form a single phase. The synthesized product was ground finely and characterized by powder X-ray diffraction. The X-ray diffraction pattern confirmed that the synthetic $Sr_5(PO_4)_3F$ is a single phase (Swafford and Holt 2002).

The high-pressure Raman measurements were performed using a symmetric type of diamond anvil cell (DAC) with a pair of 500-μm culet diamond anvils. The experimental method used in this study was similar to previous study (Shi et al. 2012). A stainless steel plate with an initial thickness of 250 μm was used as gasket. The central area of the gasket was pre-indented to a thickness of about 30 μm, and a hole of 100 μm in diameter was drilled at the center. The synthetic sample was loaded into the sample chamber, with Ar as the pressure medium. Ruby (Cr^{3+} doped α-Al_2O_3) spheres as pressure marker were carefully placed inside the gasket sample chamber. The sample pressures were determined by the ruby fluorescence method (Mao et al. 1978). Micro-Raman spectra were collected by a custom-built Raman system at University of Western Ontario. An argon-ion laser with a wavelength of 514.5 nm was used as exciting source, and a spectrometer with a liquid nitrogen-cooled CCD detector was used to collect the Raman data. The spectrometer was calibrated using a neon lamp, and the precision of the frequency determination was about 1 cm^{-1}. The data collection time was typically 120 s for each spectrum. The spectrometer position was tuned to 530 nm to collect lattice, bending (ν_2 and ν_4) modes and to 537 nm for the stretching (ν_1 and ν_3) modes. The Raman shift of each band was obtained by Lorentzian curve fitting to get a reasonable approximation by using PeakFit program (SPSS Inc., Chicago).

Results and discussion

Raman spectrum at ambient conditions

Stronadelphite is in hexagonal structure with space group of $P6_3/m$ and $Z = 2$, which is same as fluorapatite. In the structure of $Sr_5(PO_4)_3F$, two kinds of Sr^{2+} cations exist including Sr1 located on a threefold axis with nine coordinates and Sr2 in distorted pentagonal bipyramidal geometry with one bond to F and six oxygen neighbors. The phosphorous is in tetrahedrally coordinated geometry with the central P atom. The details of the crystal structure of $Sr_5(PO_4)_3F$ were given by Swafford and Holt (2002).

Previous study shows that an isolated $(PO_4)^{3-}$ free ion has T_d symmetry and four normal modes of vibration: $A_1(\nu_1) = 938\ cm^{-1}$, $E(\nu_2) = 420\ cm^{-1}$, $T_2(\nu_3) = 1017\ cm^{-1}$, and $T_2(\nu_4) = 567\ cm^{-1}$, where the species E vibrations are doubly degenerate and T_2 vibrations are triply degenerate (Griffith 1969). The effect of the crystal field of the stronadelphite lattice on internal vibrational modes may be understood by considering the phosphate site symmetry since the T_d symmetry of a free tetrahedral PO_4 is reduced to C_s in the crystal lattice. This symmetry change partially removes the degeneracies of the vibrational wave functions which would have characterized free PO_4 (Bonner et al. 2014). Studies of the vibrational properties of fluorapatite $Ca_5(PO_4)_3F$ under high pressures have been reported (Williams and Knittle 1996; Comodi et al. 2001a). According to the factor group analysis based on the $P6_3/m$ space group (C_{6h}^2), the $Sr_5(PO_4)_3F$ structure yields the same Raman active vibrations of $Ca_5(PO_4)_3F$, as following:

$$\Gamma = 12A_g + 16E_{1g} + 26E_{2g}.$$

Therefore, totally 54 Raman vibrational modes are predicted. Among these, the phosphate tetrahedron will share the following internal modes (Klee 1970):

$$\Gamma\ (PO_4\ \text{internal}) = 6A_g + 3E_{1g} + 6E_{2g}.$$

The external modes include translation vibrations and PO_4 libration vibrations. Their irreducible representations can be expressed as:

$$\Gamma\ (PO_4\ \text{translations}) = 5A_g + 3E_{1g} + 6E_{2g}.$$

$$\Gamma\ (PO_4\ \text{librations}) = A_g + 2E_{1g} + E_{2g}.$$

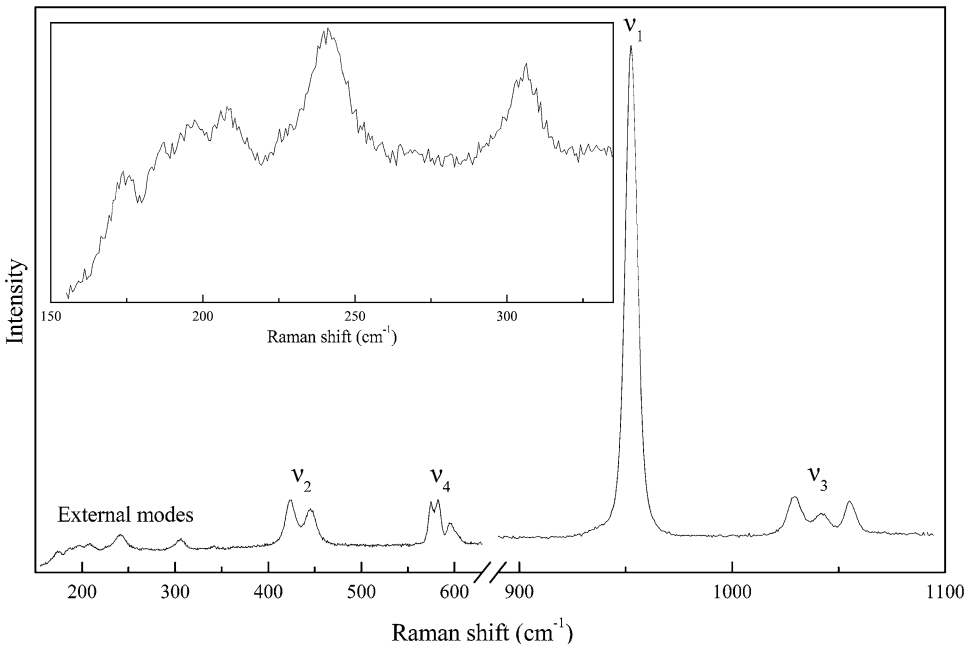

Fig. 1 Raman spectrum of $Sr_5(PO_4)_3F$ at ambient conditions. The *insert plot* shows the enlarged Raman spectrum between 150 and 335 cm^{-1}

The Raman spectrum of $Sr_5(PO_4)_3F$ at ambient condition is shown in Fig. 1. Due to the very low intensity of some modes, the number of observed Raman vibrations is fewer than predicted. The Raman spectrum was not analyzed by full range from 150 to 1100 cm^{-1}, but by four separated ranges of 150–350, 370–620, 900–1000, and 1000–1100 cm^{-1} using PeakFit Program. Therefore, the peaks can be located well. In Fig. 1, ten Raman active vibrations can be attributed to the phosphate internal modes: 423 and 445 cm^{-1} for ν_2 bending modes; 575, 582, 595, and 603 cm^{-1} for ν_4 bending modes; 952 cm^{-1} for ν_1 symmetric stretching modes; and 1029, 1042, and 1055 cm^{-1} for ν_3 asymmetric stretching modes. These typical bands are consistent with previous study reported by Schulte et al. (1995). The Davydov splitting of ν_3 and ν_4 vibrations was observed in stronadelphite, which is similar to fluorapatite (Williams and Knittle 1996). Additionally, six Raman active vibrations can be attributed to the external modes: 174, 186, 196, 208, 241, and 305 cm^{-1}. Compared with the bands of $Ca_5(PO_4)_3F$, the Raman peaks of $Sr_5(PO_4)_3F$ shift to lower frequencies. This is reasonable. The frequency of a Raman band is dependent on lattice vibrations, the masses of the atoms/ions, and the strength of the forces between the atoms/ions. According to Szigeti relationship (Parker and Seddon 1992), the frequency of the vibration, f, can be described classically by a harmonically oscillating ball and spring model as:

$$f = \frac{1}{c}\sqrt{\frac{k}{\mu}}$$

where c is the velocity of light in a vacuum (2.998×10^8 m s^{-1}), k is the bond force constant (typically in N m^{-1}), and μ is the reduced mass of the two bonding atoms [equal to $m_{1*}\, m_2/(m_1 + m_2)$]. As the bond strengths of Ca–O and Sr–O are similar (Kerr 2008), k would be expected to be similar for both bonds. Therefore, as Ca is substituted by Sr, μ will increase and f decrease, hence the Raman shift to lower values as PO_4 associated with heavier Sr cation (O'Donnell et al. 2008).

Pressure dependence of Raman spectra

High-pressure Raman spectra of $Sr_5(PO_4)_3F$ were collected up to 21.1 GPa. The typical Raman spectra of $Sr_5(PO_4)_3F$ at high pressures are reproduced in Fig. 2. It is obvious that with pressure increasing, the Raman peaks of $Sr_5(PO_4)_3F$ gradually shift to higher frequencies, which indicates a decreasing bond length of phosphate tetrahedron and metal polyhedron. This is reasonable since the P–O and Sr–O bond lengths become shorter with increasing pressure, and shorter bond lengths imply stronger bonds, i.e., larger force constant, and consequently higher vibrational frequency according to Hooke's law.

It is noted that some bands become undistinguished due to the weak intensity during compression. On the other hand, two new splittings of $Sr_5(PO_4)_3F$ were observed during compression to 10.0 and 11.8 GPa, i.e., the bands of $\nu_{4b}(A_g)$ and $\nu_{3b}(A_g)$, which was not observed in previous high-pressure Raman study of $Ca_5(PO_4)_3F$ (Williams and Knittle 1996). It should be pointed out that the peak assignment was made based on previous studies of powder sample $Ca_5(PO4)_3F$ reported by Williams and Knittle (1996) and single crystal $Ca_5(PO4)_3F$ reported by Comodi et al. (2001a). The splitting increased during compression,

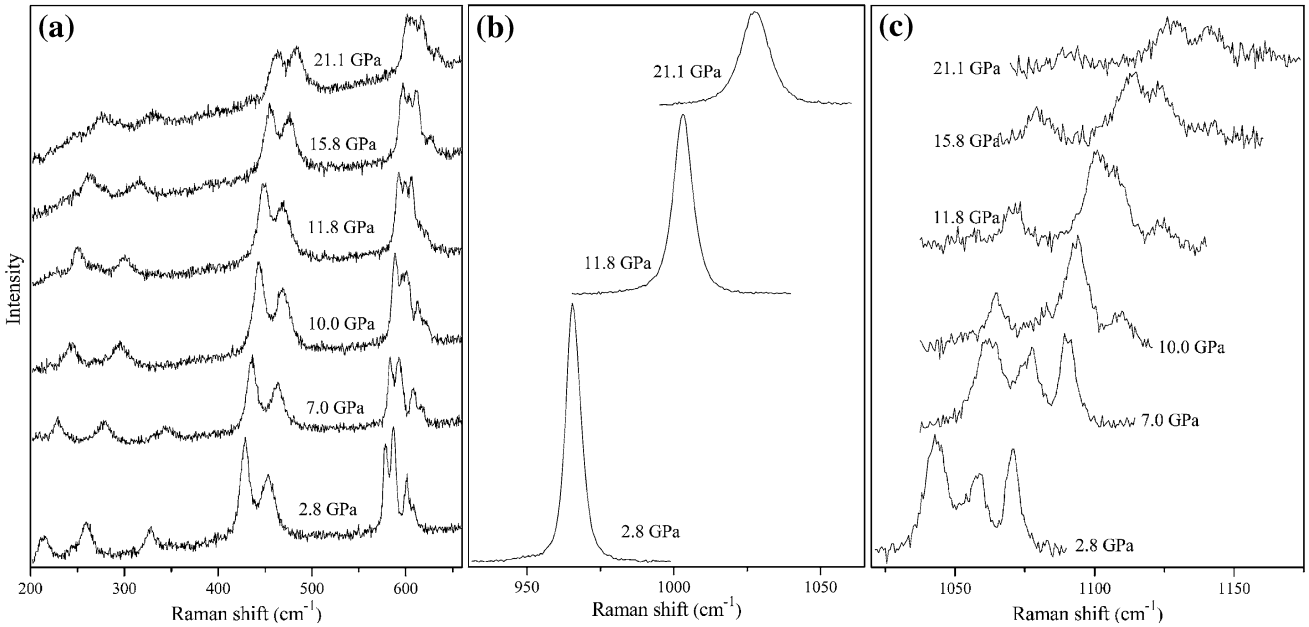

Fig. 2 Typical Raman spectra of $Sr_5(PO_4)_3F$ at high pressures and room temperature

as illustrated in Fig. 3a. The splitting of $\nu_{3b}(A_g)$ asymmetric stretching mode is more sensitive to pressure than that of $\nu_{4b}(A_g)$ bending mode. In previous high-pressure Raman study of $Ca_5(PO_4)_3F$, the mergings of $\nu_4(E_{2g})$ and $\nu_3(E_{2g})$ Davydov splittings were observed during compression, which is probably due to the change of PO_4 tetrahedra at high pressure (Williams and Knittle 1996). Figure 3b illustrates the changes of Davydov splittings in $Sr_5(PO_4)_3F$ during compression. The Davydov splittings in $Sr_5(PO_4)_3F$ do not show obvious decreases, which are different from that of $Ca_5(PO_4)_3F$ (Williams and Knittle 1996). The reason maybe is that the local crystal field surrounding the PO_4 groups in $Sr_5(PO_4)_3F$ and $Ca_5(PO_4)_3F$ is different, as described by (Bonner et al. 2014), though there is no information about the evolution of PO_4 tetrahedra in the crystal structure of $Sr_5(PO_4)_3F$ under high pressure. Previous study shows that in fluorapatite, although the average P–O bond length decreases with increasing pressure, some P–O bond lengths decrease and then increase, and the tetrahedral angle variance increases and then decreases during compression (Comodi et al. 2001b). The information about the evolution of PO_4 tetrahedra in $Sr_5(PO_4)_3F$ during compression is required to clarify the new splittings and Davydov splittings under high pressure.

The Raman shift *versus* pressure plot of $Sr_5(PO_4)_3F$ is illustrated in Fig. 4. It is noted that due to the relatively low intensities of external vibrations of $Sr_5(PO_4)_3F$ during compression, it is difficult to determine the external modes below 200 cm^{-1} under high pressures precisely. Therefore, the changes in external vibrations below 200 cm^{-1} of $Sr_5(PO_4)_3F$ at high pressures are not considered in this study. The Raman shifts of PO_4 internal modes in $Sr_5(PO_4)_3F$ change linearly and continuously with pressure, and the slopes are different for different modes.

As listed in Table 1, the pressure coefficients (β) of vibrations in $Sr_5(PO_4)_3F$ indicate that ν_3 and ν_1 stretching modes in the high-frequency region are more sensitive to pressure compared to the ν_4 and ν_2 bending modes in the low-frequency region. In fact, the pressure coefficients of ν_3 and ν_1 modes in $Sr_5(PO_4)_3F$ are 3.33–5.20 and 3.77 cm^{-1}/GPa, whereas the coefficients for ν_4 and ν_2 modes in $Sr_5(PO_4)_3F$ are 1.35–1.75 and 1.87–1.96 cm^{-1}/GPa, respectively. Meanwhile, the external modes show the largest pressure coefficient, which maybe is partially due to the more compressible of strontium polyhedra compared to PO_4 tetrahedra, as deduced from the results of $Ca_5(PO_4)_3F$ (Comodi et al. 2001b). The changes in pressure coefficients for different modes of $Sr_5(PO_4)_3F$ are similar to those of some other phosphates including $Ca_5(PO_4)_3F$, γ-$Ca_3(PO_4)_2$, $Sr_3(PO_4)_2$, $Ba_3(PO_4)_2$, and β-$Ca_3(PO_4)_2$ (Williams and Knittle 1996; Comodi et al. 2001a; Zhai et al. 2010, 2011a, 2015).

The pressure coefficients of the different Raman modes can be used to obtain the Grüneisen parameters. Based on previous result of the isothermal bulk modulus of $Sr_5(PO_4)_3F$ (He et al. 2013), the isothermal mode Grüneisen parameters, γ_{iT}, can be determined by following expressions (Gillet et al. 1989):

$$\gamma_{iT} = K_T(\partial ln\, \nu_i/\partial P)_T$$

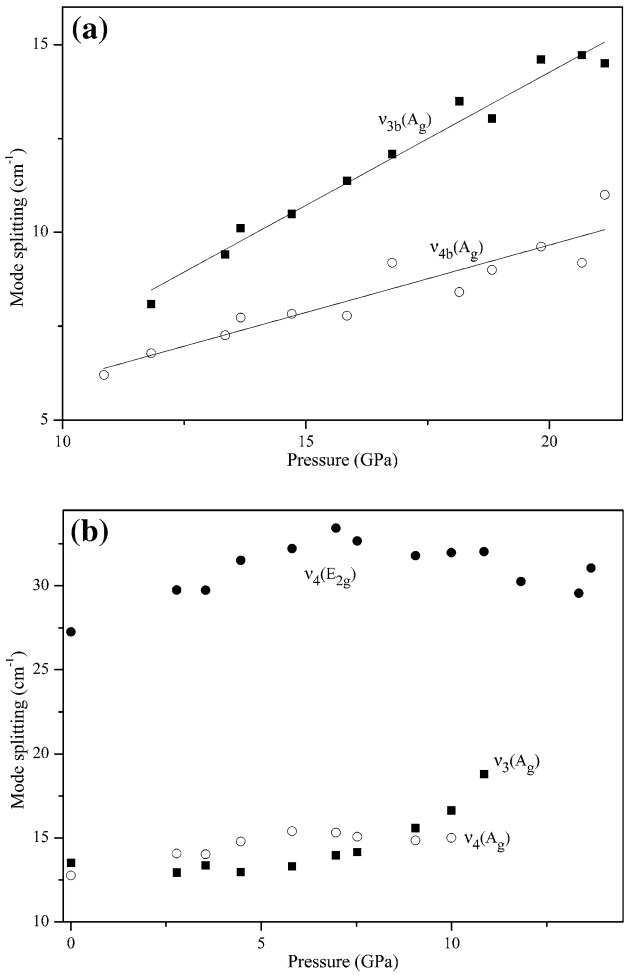

Fig. 3 Shift in splittings of the Raman bands in $Sr_5(PO_4)_3F$ during compression at room temperature. **a** Splittings of $\nu_{3b}(A_g)$ and $\nu_{4b}(A_g)$ modes **b** Davydov splittings of $\nu_4(E_{2g})$, $\nu_3(A_g)$, and $\nu_4(A_g)$ vibrations

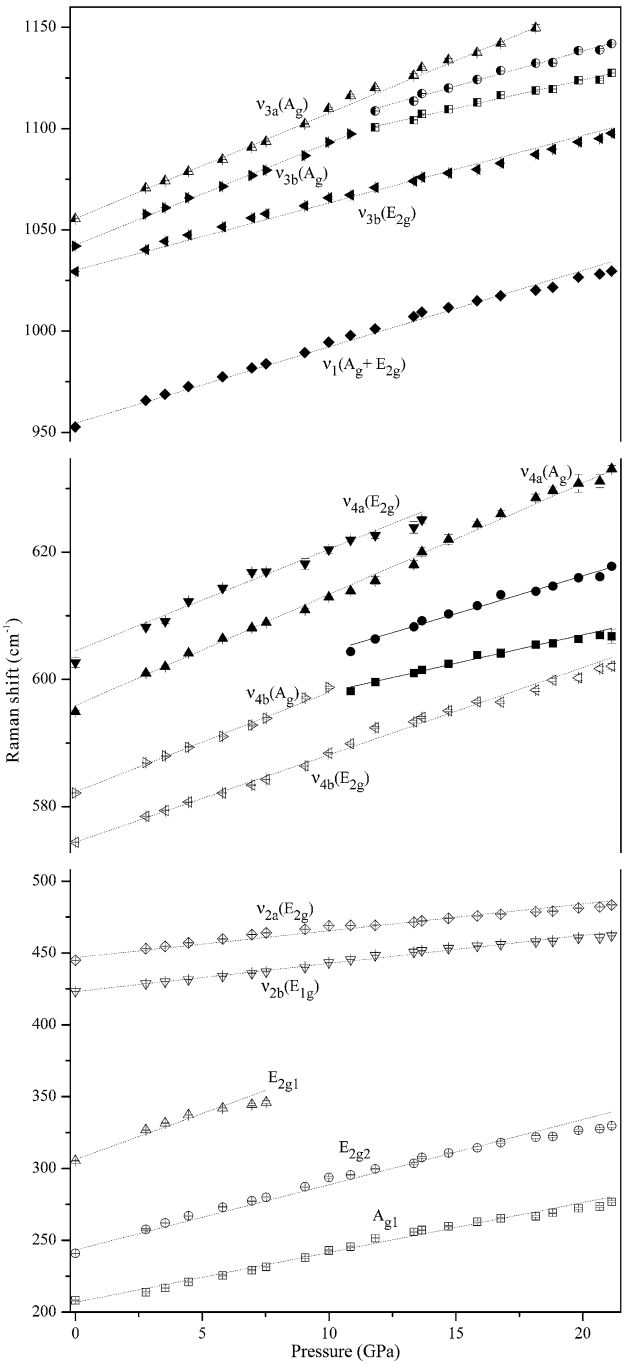

Fig. 4 Pressure dependence of the Raman bands of $Sr_5(PO_4)_3F$ at room temperature

where ν_i is the vibrational frequency of the ith band and K_T is the isothermal bulk modulus. The values of γ_{iT} for different modes of $Sr_5(PO_4)_3F$ are shown in Table 1.

An average γ_{iT} value of 0.332 can be determined for the PO_4 modes in stronadelphite, which is similar to previous study of PO_4 modes in some other phosphate minerals including fluorapatite (0.358, Williams and Knittle 1996; and 0.445, Comodi et al. 2001a), tuite (0.363, Zhai et al. 2010), whitlockite (0.343, Zhai et al. 2015), and $Sr_3(PO_4)_2$ [0.303, calculated by using reported results of Zhai et al. (2011a, b)]. The difference in average γ_{iT} value partly reflects a difference in compressibility, which is confirmed by high-pressure experimental studies (Brunet et al. 1999; Comodi et al. 2001b; Zhai and Wu 2010; He et al. 2013; Zhai et al. 2011a, b, 2013). Compared with SiO_4 modes in some silicate minerals (Gillet et al. 1992, 1997), PO_4 modes in phosphate minerals show lower average isothermal mode Grüneisen parameters, which is reasonable since phosphates are more compressible than silicates.

The bulk thermochemical Grüneisen parameter, which is equal to $\alpha KV/C_v$ (where α is the thermal expansion, K is the bulk modulus, V is the molar volume, and C_v is the volume constant heat capacity), is not available for stronadelphite

Table 1 Constants determined in the expressions of $\nu_P = \nu_{i0} + \beta P$ and $\gamma_{iT} = K_T (\partial \ln \nu_i / \partial P)_T$ for stronadelphite

	ν_0 (cm^{-1})	ν_{i0} (cm^{-1})	β (cm^{-1}/GPa)	R^2	γ_{iT}
PO_4 modes					
ν_3		1068.8 (24)	3.47 (15)	0.982	0.296
		1068.0 (16)	2.80 (1)	0.987	0.239
	1055	1055.5 (3)	5.20 (6)	0.988	0.449
	1042	1042.4 (4)	5.05 (7)	0.998	0.441
	1029	1030.0 (7)	3.33 (3)	0.994	0.295
ν_1	953	954.5 (8)	3.77 (7)	0.993	0.360
ν_4	603	604.5 (6)	1.60 (7)	0.978	0.241
	595	595.8 (3)	1.75 (3)	0.980	0.268
		592.5 (8)	1.19 (5)	0.980	0.183
		589.1 (6)	0.90 (4)	0.979	0.139
	582	582.3 (2)	1.57 (4)	0.990	0.246
	574	574.5 (2)	1.35 (2)	0.991	0.214
ν_2	445	446.8 (7)	1.87 (7)	0.972	0.381
	423	423.1 (3)	1.96 (4)	0.993	0.422
Lattice modes					
	305	306.2 (15)	6.41 (42)	0.975	1.91
	242	243.3 (10)	4.54 (12)	0.985	1.70
	208	206.9 (11)	3.47 (9)	0.985	1.53

ν_0 is observed frequency at ambient conditions. R^2 is the correlation coefficient. Grüneisen parameter γ_{iT} was calculated with isothermal bulk modulus of $K_T = 91.1$ GPa reported by He et al. (2013)

due to the lack of volume constant heat capacity. However, previous study shows that the bulk Grüneisen parameters are usually in the range from 0.8 to 2 for incompressible oxide compounds without polymerized tetrahedra (Shankland and Bass 1988). In fact, the evolution of the PO_4 tetrahedral modes is not representative of the whole structural evolution of $Sr_5(PO_4)_3F$. The external modes including the vibrations associated with the strontium polyhedra in stronadelphite can strongly affect the bulk Grüneisen parameter. As listed in Table 1, the available Grüneisen parameters of the external modes are greatly larger than those of PO_4 internal modes. Similar results were obtained for fluorapatite because the behavior of a Ca–O polyhedron is much less rigid than that of the PO_4 tetrahedron under high pressure (Comodi et al. 2001b). Therefore, for stronadelphite and other phosphates, the relatively low average value of the PO_4 mode Grüneisen parameters indicates that the lattice modes related to divalent cation displacements largely contribute to the bulk Grüneisen parameter.

Acknowledgements We thank Professor T. Tsuchiya for his editorial handling. Critical comments and suggestion from two anonymous reviewers are helpful to improve the manuscript. This work was financially supported by National Natural Science Foundation of China (Grant Nos. 41372040 and 41202020) and by National Science and Engineering Research Council of Canada.

References

Biagioni C, Pasero M (2013) The crystal structure of johnbaumite, $Ca_5(AsO_4)_3OH$, the arsenate analogue of hydroxylapatite. Am Miner 98:1580–1584

Bonner CE, Chess CC, Meegoda C, Stefanos S, Loutts GB (2014) Volume effects on the Raman frequencies of phosphate ions in fluorapatite crystals. Opt Mater 26:17–22

Brinier A (2001) A new evaluation of Yb^{3+}-doped crystals for laser applications. J Lumin 92:199–204

Brunet F, Allan DR, Redfern SAT, Angel RJ, Miletich R, Reichmann HJ, Sergent J, Hanfland M (1999) Compressibility and thermal expansivity of synthetic apatites, $Ca_5(PO_4)_3X$ with X=OH, F and Cl. Eur J Miner 11:1023–1035

Comodi P, Liu Y, Frezzotti ML (2001a) Structural and vibrational behaviour of fluorapatite with pressure. Part II: in situ micro-Raman spectroscopic investigation. Phys Chem Miner 28:225–231

Comodi P, Liu Y, Zanazzi PF, Montagnoli M (2001b) Structural and vibrational behaviour of fluorapatite with pressure. Part I: in situ single-crystal X-ray diffraction investigation. Phys Chem Miner 28:219–224

DeLoach LD, Payne SA, Smith LK, Kway WL, Krupke WF (1994) Laser and spectroscopic properties of $Sr_5(PO_4)_3F$:Yb. J Opt Soc Am B 11:269–276

Fang HS, Qiu SR, Zheng LL, Schaffers KI, Tassano JB, Caird JA, Zhang H (2008) Optimization of the cooling profile to achieve crack-free Yb:S-FAP crystals. J Cryst Growth 310:3825–3832

Gillet P, Guyot F, Malezieux JM (1989) High-pressure, high-temperature Raman spectroscopy of Ca_2GeO_4 (olivine form): some insights on anharmonicity. Phys Earth Planet Inter 58:141–154

Gillet P, Fiquet G, Maldzieux JM, Geiger C (1992) High-pressure and high-temperature Raman spectroscopy of end-member garnets: pyrope, grossular and andradite. Eur J Miner 4:651–664

Gillet P, Daniel I, Guyot F (1997) Anharmonic properties of Mg_2SiO_4-forsterite measured from the volume dependence of the Raman spectrum. Eur J Miner 9:255–262

Gloster LAW, Cormont P, Cox AM, King TA, Chai BHT (1998) Diode-pumped Q-switched Yb:S-FAP laser. Opt Commun 146:177–180

Griffith W (1969) Raman spectroscopy of minerals. Nature 224:264–266

He Q, Liu X, Li B, Deng L, Chen Z, Liu X, Wang H (2013) Expansivity and compressibility of strontium fluorapatite and barium fluorapatite determined by in situ X-ray diffraction at high-T/P conditions: significance of the M-site cations. Phys Chem Miner 40:349–360

Hughes JM, Rakovan J (2002) The crystal structure of apatite, Ca5(PO4)3(F, OH, Cl). Rev Miner Geochem 48:1–12

Huminicki DMC, Hawthorne FC (2002) The crystal chemistry of the phosphate minerals. Rev Miner Geochem 48:123–253

Kampf AR, Housley RM (2011) Fluorphosphohedyphane, $Ca_2Pb_3(PO_4)_3F$, the first apatite supergroup mineral with essential Pb and F. Am Miner 96:423–429

Kerr JA (2008) CRC Handbook of Chemistry and Physics, 81st edn. CRC Press, Florida

Khomyakov AP, Kulikova IM, Rastsvetaeva PK (1997) Fluorcaphite, Ca(Sr, Na, Ca)(Ca, Sr, Ce)$_3$(PO_4)$_3$F—a new mineral with the apatite structure motif. Zap Vser Miner Obshch 126:87–97

Klee W (1970) The vibrational spectra of the phosphate ions in fluorapatite. Zeit Kristallogr 131:95–102

Klevtsova RF (1964) About the crystal structure of strontiumapatite. Z Strukt Khim 5:318–320

Kreidler ER, Hummel FA (1970) The crystal chemistry of apatite: structure fields of fluor- and chlorapatite. Am Miner 55:170–184

Mao HK, Bell PM, Shaner JW, Steinberg DJ (1978) Specific volume measurements of Cu, Mo, Pd and Ag and calibration of the ruby R_1 fluorescence pressure gauge from 0.06 to 1 Mbar. J Appl Phys 49:3276–3283

Nagpure IM, Dhoble SJ, Mohapatra M, Kumar V, Pitale SS, Ntwaeaborwa OM, Godbole SV, Swart HC (2011) Dependence of Eu^{3+} luminescence dynamics on the structure of the combustion synthesized $Sr_5(PO_4)_3F$ host. J Alloys Compd 509:2544–2551

O'Donnell MD, Fredholm Y, de Rouffignac A, Hill RG (2008) Structural analysis of a series of strontium-substituted apatites. Acta Biomater 4:1455–1464

Pan Y, Fleet ME (2002) Compositions of the apatite-group minerals: substitution mechanisms and controlling factors. Rev Miner Geochem 48:13–49

Parker JM, Seddon AB (1992) Infrared-transmitting optical fibres. In: Cable M, Parker JM (eds) High-performance glass. Blackie, London, pp 252–286

Pasero M, Kampf AR, Ferraris C, Pekov IV, Rakovan J, White TJ (2010) Nomenclature of the apatite supergroup minerals. Eur J Miner 22:163–179

Pekov IV, Britvin SN, Zubkova NV, Pushcharovsky DY, Pasero M, Merlino S (2010) Stronadelphite, $Sr_5(PO_4)_3F$, a new apatite-group mineral. Eur J Miner 22:869–874

Qiao X, Seo HJ (2014) Luminescence and crystallographic sites for Eu^{3+} ions in $Sr_5(PO_4)_3F$ phosphor. J Alloys Compd 615:270–275

Schaffers KI (2004) Yb:S-FAP lasers. Opt Mater 26:391–394

Schulte A, Buchter S, Chai B (1995) Raman spectroscopy of fluorophosphate and fluorovanadate laser crystals. Proc Soc Photo Opt Instrum Eng 2380:34–42

Shankland TJ, Bass JD (1988) Elastic properties and equations of state. American Geophysical Union, Washington, DC

Shi WG, Fleet ME, Shieh SR (2012) High-pressure phase transitions in Ca–Mn carbonates (Ca, Mn)CO3 studied by Raman spectroscopy. Am Miner 97:999–1001

Swafford SH, Holt EM (2002) New synthetic approaches to monophosphate fluoride ceramics: synthesis and structural characterization of $Na_2Mg(PO_4)F$ and $Sr_5(PO_4)_3F$. Solid State Sci 4:807–812

Wang Q, Zhao S, Zhang X, Sun L, Zhang S (1996) Laser demonstration of a diode-laser-pumped Nd:$Sr_5(PO_4)_3F$ crystal. Opt Commun 128:73–75

White T, Ferraris C, Kim J, Madhavi S (2005) Apatite- An adaptive framework structure. Rev Mineral Geochem 57:307–401

Williams Q, Knittle E (1996) Infrared and raman spectra of $Ca_5(PO_4)_3F$-flurapatite at high pressures: compression-induced changes in phosphate site and Davydov splitting. J Phys Chem Solid 57:417–422

Zhai S, Wu X (2010) X-ray diffraction study of β-$Ca_3(PO_4)_2$ at high pressure. Solid State Commun 150:443–445

Zhai S, Wu X, Ito E (2010) High-pressure Raman spectra of tuite, γ-$Ca_3(PO_4)_2$. J Raman Spectrosc 41:1011–1013

Zhai S, Liu A, Xue W, Song Y (2011a) High-pressure Raman spectroscopic studies on orthophosphates $Sr_3(PO_4)_2$ and $Ba_3(PO_4)_2$. Solid State Commun 151:276–279

Zhai S, Xue W, Yamazaki D, Shan S, Ito E, Tomioka N, Shimojuku A, Funakoshi K (2011b) Compressibility of strontium orthophosphate $Sr_3(PO_4)_2$ at high pressure. Phys Chem Miner 38:357–361

Zhai S, Yamazaki D, Xue W, Ye L, Xu C, Shan S, Ito E, Yoneda A, Yoshino T, Guo X, Shimojuku A, Tsujino N, Funakoshi K (2013) P-V-T relations of γ-$Ca_3(PO_4)_2$ tuite determined by in situ X-ray diffraction in a large-volume high-pressure apparatus. Am Miner 98:1811–1816

Zhai S, Wu X, Xue W (2015) Pressure-dependent Raman spectra of β-$Ca_3(PO_4)_2$ whitlockite. Phys Chem Miner 42:303–308